Materials and Design 172 (2019) 107763

Contents lists available at ScienceDirect

Materials and Design

journal homepage: www.elsevier.com/locate/matdes

Mechanical property enhancement of self-bonded natural fiber material via controlling cell wall plasticity and structure

Quanliang Wang [a], Shengling Xiao [a,*], Sheldon Q. Shi [b], Liping Cai [b]

[a] College of Engineering and Technology, Northeast Forestry University, Harbin 150040, China
[b] Department of Mechanical and Energy Engineering, University of North Texas, Denton, TX 76203, USA

HIGHLIGHTS

- High-performance self-bonded natural fiber material was developed using pulp fibers that were made from hardwood wastes
- Mechanical property was enhanced through comprehensive treatments on fiber cell wall plasticity and structures
- Establishment of functions among mechanical strength, lignin content, hemicellulose content and mat moisture content
- Comparison with plastic and wood confirmed the mechanical strength superiority of self-bonded natural fiber material

GRAPHICAL ABSTRACT

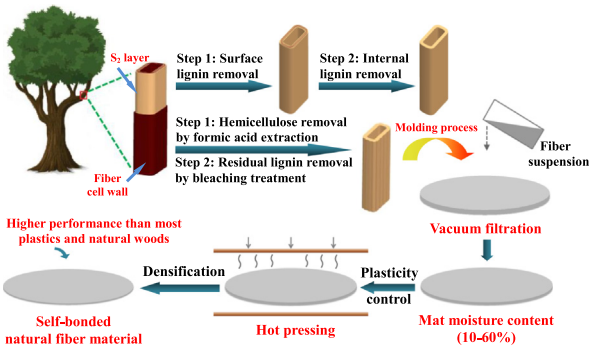

ARTICLE INFO

Article history:
Received 18 February 2019
Received in revised form 25 March 2019
Accepted 25 March 2019
Available online 26 March 2019

Keywords:
Natural fiber
Self-bonded
Fiber cell wall
Mechanical property

ABSTRACT

Self-bonded natural fiber material (SNFM) is a promising alternative for plastic and wood owing to its abundant raw material resources and low environmental impact. In this study, a high-performance SNFM was developed by the comprehensive treatments for the plasticity and structure of fiber cell walls. The cell wall structure was treated by a progressive chemical etching process for selectively removing surface lignin, internal lignin and hemicelluloses, respectively. The cell wall plasticity was tuned by controlling the fiber moisture content during compression molding process. The results showed that the increase in fiber plasticity improved the tensile strength from 38.0 to 83.5 MPa and the flexural strength from 31.2 to 73.3 MPa. The selective removal of surface lignin increased the flexural strength from 101.3 to 122.1 MPa. The functional relationships among mechanical strength, lignin content, hemicellulose content and moisture content were established. The self-bonded mechanism for natural fiber materials was also discussed. The SNFM products showed excellent mechanical performance (tensile strength: 21.5–83.5 MPa; flexural strength: 31.2–127.3 MPa), which was superior to that of natural wood (46.5–55.6 MPa; 70.7–92.4 MPa) and plastic (15.9–51.0 MPa; 21.7–73.0 MPa) (e.g., HDPE, PP, PVC, and ABS).

1. Introduction

High-performance self-bonded natural fiber material (SNFM) is a new kind of cellulosic fiber material, which is characterized by the usage of high lignin content of natural fibers as the start material, and exhibits excellent mechanical properties differed from traditional

* Corresponding author.
E-mail address: shenglingxiao@126.com (S. Xiao).

https://doi.org/10.1016/j.matdes.2019.107763

molded pulp materials by the self-bonding [1]. SNFM is considered as a promising alternative to other structural materials (e.g., plastic and natural wood) in building and related applications due to its advantages of eco-friendliness, cost-effectiveness, and scalability [2]. Natural fiber materials can be fabricated from the abundant and low-cost agricultural and forestry crops, such as straws, corn stalk, kenaf, and wood waste [3–5]. However, large amounts of crop straws and wood wastes are abandoned every year due to their low costs for current applications. Thus, it is of great significance to produce eco-friendly and high-performance SNFM products using these types of feedstock. Compared to traditional natural fiber-based composites (e.g., glued fiberboard and fiber-reinforced composites) with complexity in industrial production, hazards to human health, and non-recyclability [6], the SNFM products can produce excellent mechanical performance through a facile compression molding process, and present eco-friendly, harmless and recyclable characteristics [7].

Natural fiber products can be self-bonded by the inter-fiber physical contact and cross-linking, and the interfacial bonding between fiber cell walls. Unlike papermaking and pulp molding that were bonded via hydrogen bonding simply [8], SNFM can achieve the high-strength self-bonding through a reasonable design from the level of fiber cell walls. It was included the consideration in physical properties of fibers (such as tensile strength, stiffness, and plasticity), and the self-bonding design in the case of lignin distribution, microfibril exposure, and hemicellulose content in cell walls [9,10]. Obviously, SNFM has better component compatibility than fiber reinforced composites due to the direct contact between natural fibers [11]. As the basic building block in SNFM, the fiber cell wall plays an important role in determining the material strength, which is dependent on the physical property and chemical structure of fibers [12]. Thus, the raw material and fiber preparation process should be optimized for obtaining the targeted fibers. The physical contact and chemical bonding between fibers are the key factors that determine the self-bonded strength for high-performance SNFM products, which could be controlled by the compression molding parameters (e.g., fiber mat moisture content and hot-pressing temperature) [13,14]. Meanwhile, the treatment on natural fibers (such as lignin etching and grafting of functional groups) can also affect the fiber properties and the self-bonding strength.

Many approaches have been reported on the mechanical property enhancement for natural fiber-based materials, such as the additions of adhesives and inorganic particles [15–18]. Shen et al. [19] reported that the mechanical and fracture performance of ramie fiber-reinforced composites could be improved by incorporating carbon nanotubes. Loong and Cree [20] found that the bio-resin composite tensile strength, stiffness and bond shear strength could be enhanced by the acetic anhydride treated flax fibers. Dayo et al. [21] used waste hemp fibers to reinforce the polybenzoxazine composites, and revealed that the tensile strength, flexural and Young's modulus were significantly enhanced after loading hemp fibers in the polymer matrices. Wang et al. [22] reported that the grafting of nano-TiO_2 onto flax fibers could increase the interfacial shear strength to the fiber reinforced epoxy composites and demonstrated that the formation of Si—O—Ti and C—O—Si bonds and the presence of the nanoparticles contributed to the property enhancements. However, these reinforced methods have a fatal defect because the treated natural fibers in the composites are not recyclable, which thus leads to the natural fiber materials becoming disposable products after the treatment with adhesives. For the traditional self-bonded natural fiber materials, the mechanical properties are usually improved simply by the mechanical pressurization or complete removal of lignin [23,24], which is improper for producing high-performance SNFM products. Moreover, the high mechanical strength is the most important performance for SNFM applied in building and related applications [25]. Therefore, it is necessary to develop new approaches for improving the mechanical property of natural-fiber products.

Natural fibers (e.g., lignocellulosic fibers) exist in the form of tubular cell wall, which has a complex nanocomposite structure [26]. The cellulose microfibrils are arranged in a certain angle and manner, and the hemicelluloses and lignin are bonded together and filled between microfibrils in a disordered state [27,28]. The hemicelluloses are the oligomeric mixture containing various monosaccharides, which adhere to the microfibril surfaces [29]. Lignin has a structure skeleton consisting of phenylpropane, working as the rigid support in the fiber cell wall [24]. The softening point of lignin can be reduced under the presence of moisture, which thus changes the thermal plasticity of lignin [30]. Much work has been reported on the plasticity of isolated lignin, but the plasticity of fiber cell walls for the application in mechanical property reinforcement has not been reported yet. A complete delignification treatment is usually adopted for enhancing mechanical properties by the hydrogen bonding [31]. Obviously, the physical property (e.g., plasticity) and chemical structure (e.g., lignin distribution and hemicellulose content) of fiber cell wall are not considered for the property enhancement.

In this work, it is aimed at the mechanical enhancement of SNFM products in the plasticity and structures of fiber cell wall. The moisture in fiber mat was used for the effective control on fiber plasticity during compression molding process. The quantitative etching of lignin from the cell wall surface into the core was performed by sodium chlorite treatment. The selective etching of hemicelluloses was carried out by a novel microwave-assisted formic acid (MAFA) treatment process. The mechanical properties were measured using the tensile and bending tests. The chemical changes of fibers during the plasticizing and etching (i.e., surface lignin, internal lignin, and hemicelluloses) process were characterized by the X-ray photoelectron spectroscopy (XPS), X-ray diffraction (XRD), and scanning electron microscope (SEM).

2. Materials and methods

The original fibers (OrF) of poplar waste were prepared by a chemi-thermomechanical pulping process in the laboratory. These fibers presented a mean length of 694 μm with an aspect ratio of 46, which were mainly composed of lignin (24.9%), hemicelluloses (15.7%), and cellulose (59.4%). All reagents were purchased from Sinopharm Chemical Reagent Co., Ltd., Beijing, China.

2.1. Enhancement of fiber plasticity by mat moisture

The lignin-rich fibers are difficult to be deformed plastically due to the stubbornness of lignin, which limits the inter-fiber contact and cross-linking during hot-pressing process. Thus, the moisture in fiber mat was used as a cost-effective and clean resource for the fiber plasticization.

25 g dry OrF was molded into a fiber mat in the ZT7-01 Shaper (Xingping Zhongtong Test Equipment Ltd., China), following by a pre-compression under 2 MPa at room temperature (rT) in 1 min. The wet fiber mat (moisture content ≈ 90%) was placed in a microwave oven (Midea, EG720KG3-NR1) to adjust the moisture content into certain levels (e.g., 60%, 50%, 40%, 30%, 20%, and 10%). Finally, the fiber mats with different moisture contents were separately placed into the sample bags in 24 h for water equilibrium.

2.2. Quantitative etching of lignin in fiber cell wall using sodium chlorite

Most cell wall surfaces of the original fibers were covered with lignin, showing low activity for the inter-fiber bonding. Thus, the controlled etching of lignin in fiber cell walls was performed using sodium chlorite.

20 g dry OrF, 650 ml distilled water, 5 ml glacial acetic acid, and 6 g sodium chlorite were placed in a 1000 ml conical flask, buckled with a 100 ml conical flask and kept at 75 °C by a water bath. The addition of the chemicals (i.e., 5 ml glacial acetic acid and 6 g sodium chlorite) and the 60 min thermosetting process were repeated at least three times. The delignified fibers (DF) were designated with the

delignification time in the lower case, i.e., DF_{15}, DF_{60}, DF_{120}, DF_{160} and DF_{240}. DF_0 represents the control sample, which was prepared without sodium chlorate/acetic acid, i.e., 20 g dry original fibers and 650 ml distilled water in the conical flask heating at 75 °C in 60 min.

2.3. Selective etching of hemicelluloses in fiber cell wall by microwave-assisted formic acid (MAFA) extraction

The delignified fibers were mainly composed of hemicelluloses and cellulose. Most hemicelluloses within the fibers limited the dissociation of microfibrils, which adversely affected the inter-fiber bonding. Thus, the selective etching of hemicelluloses was carried out by the MAFA process.

4 g dry OrF and 120 ml formic acid aqueous solution (88% wt) were placed in a 500 ml flask and heated in the microwave oven at 100 °C for 0.5 h, 1.5 h, and 4.0 h, respectively. The cellulose rich solid (CRS) was separated in a filtering crucible. Then the additional 120 ml formic acid solution (88%) was mixed with the separated CRS again and heated in the microwave oven at 100 °C for 0.5 h, 1.5 h, and 4 h, respectively. The CRS was further separated and mixed with 130 ml distilled water, 1.0 ml acetic acid (99.7%), and 1.5 g sodium chlorite (80%) in a 250 ml flask. The liquid mixture was heated at 75 °C for 1 h for bleaching. In the end, the hemicellulose-removed fibers (HF) were obtained after the bleached CRSs, being fully washed to neutral, which were designated with the MAFA treatment time in the lower cases, i.e., $HF_{1.0}$, $HF_{3.0}$ and $HF_{8.0}$. $HF_{0.0}$ meant the control samples, which was prepared without formic acid process, i.e., the original fibers were directly bleached for at least three times using sodium chlorite for the complete removal of lignin.

2.4. Preparation of self-bonded natural fiber material

The original fiber mats controlled with different moisture contents were hot-pressed under 12 MPa at 170 °C for 20 min. The hot-pressed OrFs were designated as Pr-OrFs with the moisture content in the lower case, i.e., Pr-$OrF_{60\%}$, Pr-$OrF_{50\%}$, Pr-$OrF_{40\%}$, Pr-$OrF_{30\%}$, Pr-$OrF_{20\%}$, and Pr-$OrF_{10\%}$.

25 g treated fibers (DFs or HFs) were molded into a fiber mat in the Shaper. The pre-compression was carried out under 2 MPa at rT for 1 min. The pre-compressed fiber mat was heated in the microwave oven and controlled at a moisture content of 60%. After water equilibrium, the wet fiber mat was hot-pressed under 8 MPa for DFs and 4 MPa for HFs at 170 °C for 20 min. The hot-pressed samples were designated as Pr-DF or Pr-HF with the same lower case nomenclature as indicated above.

2.5. Mechanical property tests of SNFM products

The density was measured in accordance with the ISO 534: 2011 standard. Specimens were placed at rT for 24 h before mechanical tests. The average value of eight measurements in each sample group was reported.

The tensile test was performed on a CMT5504 universal mechanical testing machine (Shenzhen SANS Testing Machine Co., Ltd., China) according to ISO527-3: 2018. The specimen dimension was $12 \times 150 \times 0.6\ mm^3$ (width × length × thickness). The gauge length was pre-set in 100 mm, and the crosshead speed was pre-set at $2\ mm\ min^{-1}$.

The bending test was carried out on the CMT5504 universal mechanical testing machine in accordance with the procedure described in ISO178: 2010 standard. The specimen dimension was $15 \times 100 \times 0.6\ mm^3$ (width × length × thickness). Three-point bending set-up was used with a span of 40 mm and a crosshead speed of $10\ mm\ min^{-1}$.

2.6. Chemical composition and X-ray photoelectron spectroscopy (XPS) analysis

The hemicelluloses and lignin content were determined according to GB/T 745-2003 and GB/T 747-2003 standard, respectively. The cellulose content of the delignified fibers was evaluated using Eq. (1).

$$\text{Cellulose content}\% = (1-H/C) \times 100\% \quad (1)$$

where H is the weight of hemicelluloses in the delignified fibers, and C is the weight of pulp fibers.

The composition on the fiber surface was determined by a K-Alpha X-ray photoelectron spectrometer (Thermofisher Scientific Company, USA). Before the XPS determination, SNFM samples were placed into the Soxhlet and extracted for 8 h using acetone. After air-dried for 24 h, all samples were dried at 60 °C to a constant weight. According to previous report [32], it can be considered that most extractives on the fiber surface were removed after the acetone extraction.

2.7. X-ray diffraction (XRD) analysis

The crystal structure of cellulose in fibers was investigated using an X-ray diffractometer (Rigaku D/max 2200, Japan) ranging from 5° to 40° at 40 kV and 30 mA. The crystallinity index (CrI) was calculated according to Eq. (2) [33].

$$\text{CrI}\% = (1-I_{am}/I_{200}) \times 100\% \quad (2)$$

where I_{200} is the intensity of the crystalline portion at around $2\theta = 22.8°$ and I_{am} is the intensity of the amorphous portion at $2\theta = 18°$.

2.8. Microtopography analysis

The surface and cross-section morphologies of fiber cell walls were observed by a Quanta-200 environmental scanning electron microscope (FEI Company, USA) with an accelerating voltage of 12.5 kV and a magnification of 500×, 1000× and 5000×. The cross-sections were prepared by a Feather microtome blade.

3. Results and discussion

3.1. Transition process in the plasticity and structures of fiber cell wall for SNFM preparation

The plasticity of fiber cell wall was altered by changing the mat moisture content during the hot-pressing process (Fig. 1a). The lignin-rich fibers were firstly molded into a fiber mat, then the fiber mat was

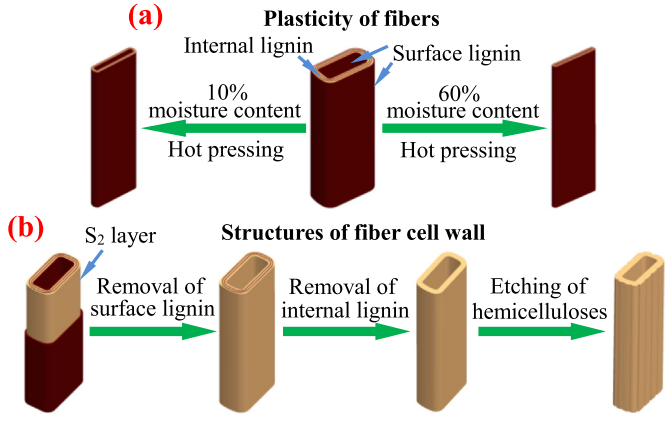

Fig. 1. Illustration of transitions of natural fiber cell wall via controlling its (a) plasticity and (b) structures.

controlled with different moisture contents before hot-pressing. The fiber plasticity was increased due to the presence of water, especially along with a decrease in the lignin softening point. It was contributed to the deformation of fiber cell wall, thus increasing the inter-fiber contact and bonding strength.

The progressive structural change of fiber cell wall was achieved by gradually etching the surface lignin, internal lignin, and hemicelluloses (Fig. 1b). Most fiber surfaces were covered by lignin. The surface lignin was firstly removed, and then the internal lignin within the cell wall was etched during the delignification process. The removal of the surface lignin changed the surface compositions and physical properties of fibers, which thus dramatically affected the interfacial bonding between fibers. The further etching of internal lignin in the fiber cell wall produced an adverse effect on the stiffness of single fibers. After the removal of residual lignin, the further etching of hemicelluloses could enhance the separation and exposure of microfibrils, which was conducive to the inter-fiber bonding, but accompanied by the destruction of the fiber cell wall structures.

3.2. Chemical composition and XPS analysis

The lignin, hemicellulose and cellulose contents of the pulp fibers before (i.e., DF_0) and after the etching treatment (i.e., DFs and HFs) are shown in Fig. 2a. With the lignin etching time from 0 to 240 min, the lignin content in fibers was decreased from 24.9% to nearly zero. Meanwhile, hemicellulose and cellulose contents were well maintained and increased accordingly, respectively. As the MAFA treatment was extended from 0 to 8.0 h, the hemicellulose was decreased from 20.4% to 6.8%. The results demonstrated that the chemical etchings via sodium chlorite and MAFA extraction could effectively control the structures of fiber cell wall.

The lignin content on the fiber surface was investigated by the XPS analysis (Fig. 2b–e). The increase in O/C values indicated the decreased lignin concentration [24]. Interestingly, the O/C value exhibited a remarkable decrease firstly before the expected increase. It can be reasoned that the bulk lignin fragments from early stages of delignification was deposited on the fiber surface. As the delignification proceeded, the lignin covered on the fiber surface was gradually dissolved and disappeared. It can be confirmed by the same O/C value (i.e., 0.53) for the Pr-DF_{120} and Pr-DF_{240}, and only the residual lignin was existed within the fiber cell walls.

The high-resolution carbon C1s peak detected on the surface of Pr-DFs was resolved into three (Fig. 2b, d and e) or four sub-peaks (Fig. 2c). The binding energy of the carbon was shifted to higher values with the increase in the number of oxygen atoms linked to carbon atoms, which were assigned to C1: C—C or C—H; C2: C—O; C3: C═O or O—C—O; and C4: O—C═O, respectively [34]. C4 was only appeared in Pr-DF_{60} with trace amount (0.7%), which indicated that the carboxylic group was appeared in the starting stage of the delignification. Importantly, the relative content of C1 representing the lignin content increased firstly from 44.6 to 54.2%, and then remained unchanged at ca. 35% during the further delignification. It was in agreement with the O/C results, and further showed the staged lignin etching process formed the outer surface firstly and then into the inside of fiber cell wall.

3.3. XRD analysis

The crystal structure and crystallinity and of treated fibers (i.e., DFs and HFs) and SNFM products (i.e., Pr-OrFs, Pr-DFs, and Pr-HFs) were analyzed by the X-ray diffraction technique. The XRD patterns are shown in Fig. 3. All the samples present a same cellulose I crystal structure, which is characterized by the peaks at around $2\theta = 14.2°$, 16.4°, and 22.4°, corresponding to (101), (101), and (200) planes, respectively [35]. It was demonstrated that the cellulose crystal type in fibers was not changed during the plasticizing and structural etching process. However, the increase in the plasticity of fibers adversely affected the crystallinity of Pr-OrFs, which was ascribed to the excessive softening of fibers and the destruction of crystalline region for the high mat moisture content during the compression molding process. As expected, the crystallinity index of treated fibers was increased from 49.2% (DF_0) to 76.0% ($HF_{8.0}$) with the progressive removal of amorphous lignin and hemicelluloses. Almost all the treated fibers exhibited an increased crystallinity after the hot-pressing treatment (Fig. 3c), which was attributable to the partial co-crystallization of crystallites in adjacent fibrils [36]. This also confirmed that the high-temperature compression molding was an effective method for the enlargement in crystalline region and the enhancement in dimensional stability for the SNFM products.

3.4. SEM analysis

The morphological changes of fibers plasticized with different mat moisture contents are shown in Fig. 4a–d. As the mat moisture content increased, the fiber cell walls showed a significant improvement in softening degree during the hot-pressing process, which can be seen by the more compact cell lumens, larger contact area between fibers, and higher density value from 0.86 g cm^{-3} for Pr-$OrF_{10\%}$ to 1.02 g cm^{-3}

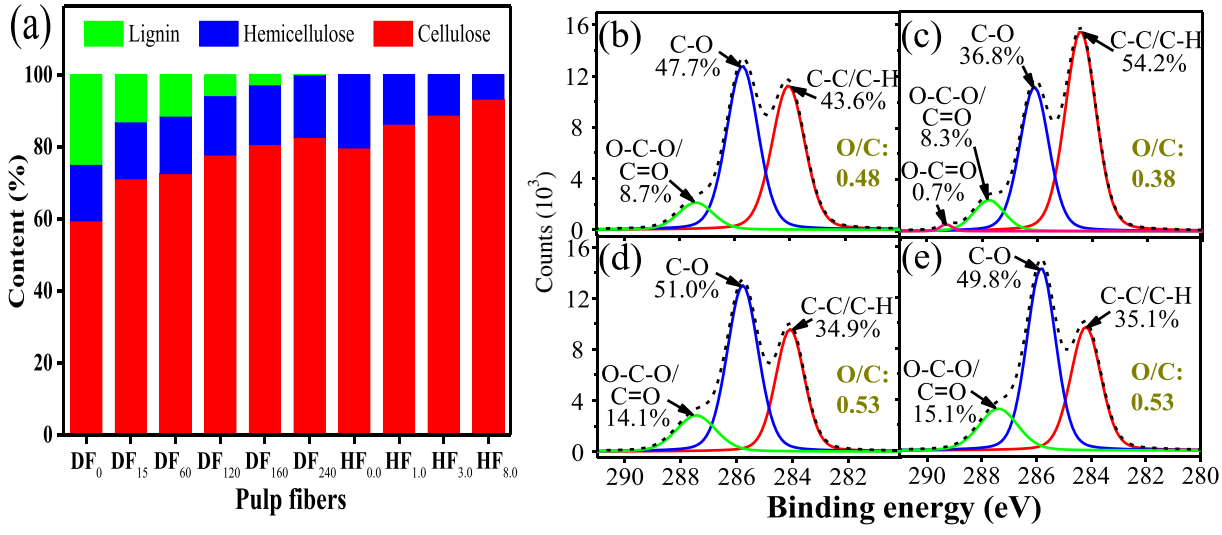

Fig. 2. Chemical composition of (a) treated fibers and C1s spectra of (b) Pr-DF_0, (c) Pr-DF_{60}, (d) Pr-DF_{120} and (e) Pr-DF_{240}.

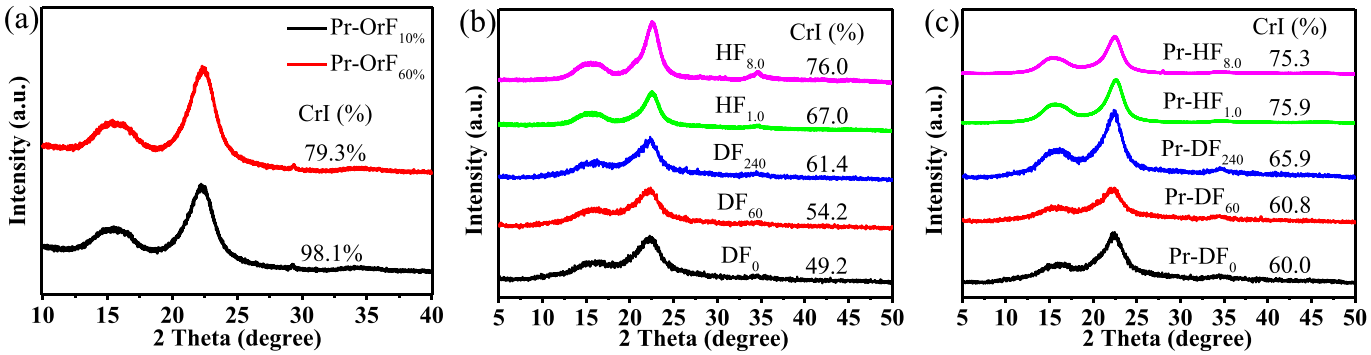

Fig. 3. XRD spectra of (a) Pr-OrFs, (b) DFs/HFs, and (c) Pr-DFs/HFs.

for Pr-OrF$_{60\%}$. It was worthy of noting that the high content of mat moisture produced a positive effect on the interfacial bonding between fibers by enhancing the lignin viscosity and hydrogen bonding during the hot-pressing process.

The microstructures of fiber cell wall during the progressive etching of lignin and hemicelluloses are shown in Fig. 4e–l. For the original fibers, it was shown a smooth and stiff appearance without exposed microfibrils due to the lignin-rich surface and presented a loose contact between fibers in the cross section. After the lignin etching treatment for 60 min, microfibrils began to be exposed on the fiber surfaces, which acted as the binder in the enhancement of inter-fiber bonding. The corresponding cross section (Fig. 4j) confirmed a dense contact between fibers, and presented a well fiber structure without significant changes in the cell wall thickness compared to that of original fibers. It was also indicated that most of the surface lignin was removed, but the internal lignin remained well for the sample of Pr-DF$_{60}$.

With the further etching of lignin to 240 min, more microfibrils were exposed on the fiber surface. However, it was still preserved a complete cell wall structure, and the contact between fibers became much more compact (Fig. 4k). According to the chemical composition and XPS analysis, it was concluded that most chemicals used for lignin etching was consumed in the degradation of lignin fragments shed in the stage of 60–120 min, and in the removal of residual lignin within fiber cell wall during 120–240 min. However, the distinguishing structural destruction on fiber cell walls was found for the further hemicellulose etching process (Fig. 4h). The broken structure of fibers allowed for a close contact between fibers with great compactness (Fig. 4l) for SNFM products. Obviously, the inter-fiber bonding was enhanced. However, the single fiber strength was reduced, which could be detrimental to the enhancement of material properties.

3.5. Effect of fiber plasticity on mechanical properties of SNFM products

The mechanical test results of the SNFM products formed at different mat moisture contents are shown Fig. 5. The thickness and density of SNFM specimens are given in Table 1. The mechanical strength of Pr-OrFs was significantly enhanced by increasing the fiber plasticity using mat moisture. Both tensile strength and flexural strength were improved with the increase of the mat moisture content, and showed a better linear goodness of fitting. As the moisture content was increased from 10 to 60%, the tensile strength increased from 38.0 to 83.5 MPa (≈120% increment), and the flexural strength increased from 31.2 to 73.3 MPa (≈135% increment). Two reasons were proposed for the increase in mechanical properties: 1) the improvement of fiber

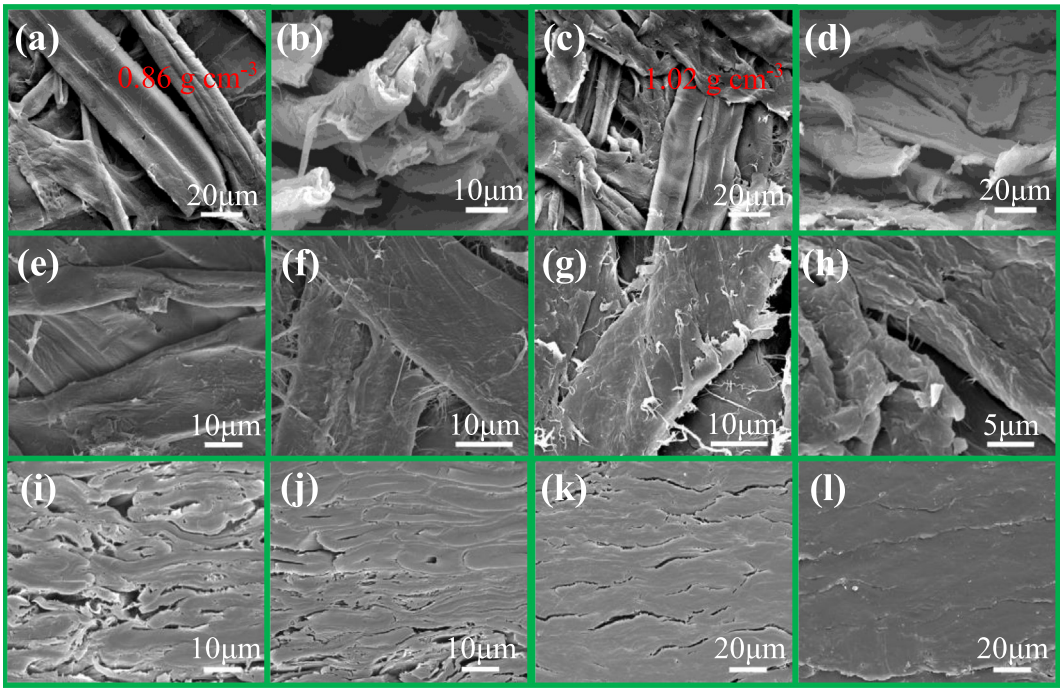

Fig. 4. SEM images of (a, b) Pr-OrF$_{10\%}$, (c, d) Pr-OrF$_{60\%}$, (e, i) Pr-DF$_0$, (f, j) Pr-DF$_{60}$, (g, k) Pr-DF$_{240}$ and (h, l) Pr-HF$_{8.0}$; (e-h) outer surface and (i-l) cross section.

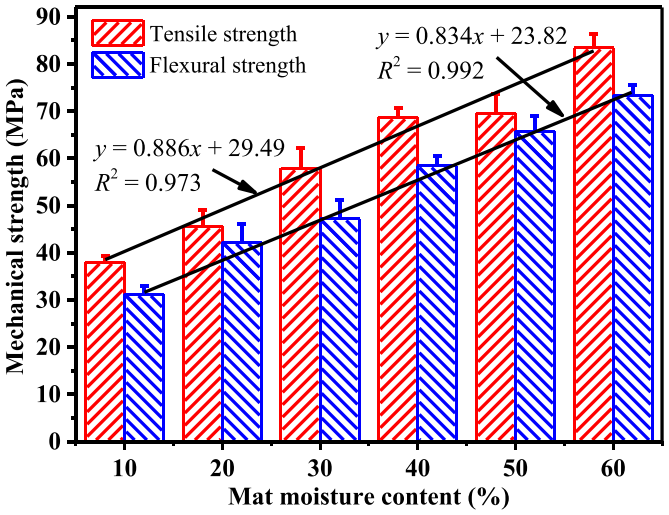

Fig. 5. Effect of mat moisture content on tensile and flexural strength of Pr-OrFs.

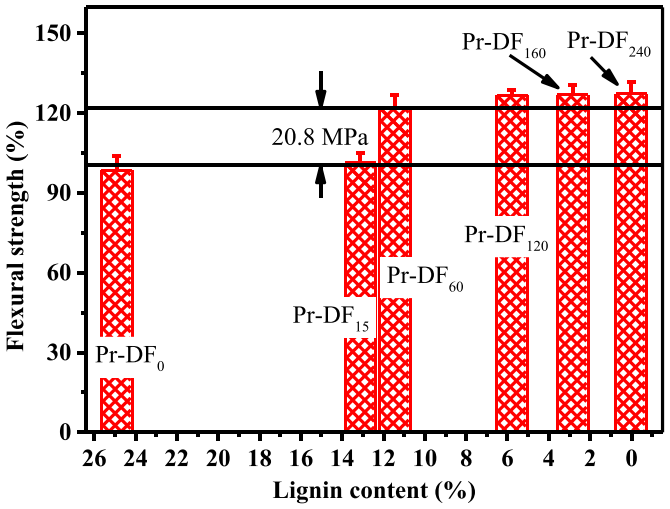

Fig. 6. Effect of lignin content on flexural strength of Pr-DFs.

plasticity increased the contact area and physical crosslinking between fibers, 2) high content of mat moisture enhanced the interfacial bonding by improving the lignin viscosity and hydrogen bonding.

3.6. Effect of fiber structures on flexural property of SNFM products during lignin etching process

The flexural strength of SNFM products is the most important mechanical performance in building and related applications, which can be improved through the lignin etching treatment. Fig. 6 shows the flexural strength of Pr-DFs fabricated by different lignin contents of fibers. It was found that only a slight increase in the flexural strength was presented with decreasing lignin content in the ranges of 0.0–11.5% and 13.1–24.9%. However, a steep increment (20.8 MPa) occurred between 13.1% and 11.5% lignin contents. From the XPS and SEM analysis, it can be explained that both the inter-fiber bonding and single fiber stiffness worked as decisive roles in affecting the flexural strength of SNFM. Compared to DF_{15} covered by large amount of lignin, DF_{60} showed that a delignified surface exposed with numerous hydroxyl groups, which led to the rapid increase in the interfacial bonding strength between fibers. Meanwhile, due to the well-maintained stiffness of single fibers, the steep enhancement in flexural strength was obtained. It was worthy of noting that the further removal of residual lignin within fibers produced an adverse effect on the stiffness of single fibers. Thus, the further enhancement in the inter-fiber bonding was only accompanied with a small increase in flexural strength between Pr-DF_{60} and Pr-DF_{240}. Thus, quantitative etching of surface lignin was of great significance to balance the bending performance and energy consumption.

Table 1
Thickness and density of SNFM products.

Specimens	Thickness (mm)	Density (g cm^{-3})
Pr-$OrF_{10\%}$	0.92 (0.05)[a]	0.86 (0.04)
Pr-$OrF_{30\%}$	0.80 (0.03)	0.96 (0.04)
Pr-$OrF_{60\%}$	0.74 (0.01)	1.02 (0.01)
Pr-DF_0	0.75 (0.02)	0.99 (0.03)
Pr-DF_{15}	0.72 (0.01)	1.03 (0.02)
Pr-DF_{60}	0.72 (0.01)	1.05 (0.02)
Pr-DF_{120}	0.69 (0.01)	1.06 (0.02)
Pr-DF_{240}	0.68 (0.01)	1.06 (0.02)
Pr-$HF_{0.0}$	0.36 (0.02)	0.91 (0.05)
Pr-$HF_{3.0}$	0.36 (0.01)	0.97 (0.04)
Pr-$HF_{8.0}$	0.30 (0.02)	0.97 (0.06)

Notes:
[a] Mean (standard deviation).

3.7. Effect of fiber structures on tensile property of SNFM products during lignin and hemicellulose etching process

A comparison of the tensile properties between Pr-DFs and Pr-HFs is shown in Fig. 7. The lignin etching treatment had a positive effect on the tensile strength of SNFM products, which was contrary to that of the hemicellulose etching process. It was found that the lower lignin content and higher hemicellulose content allowed for a higher tensile strength. As the lignin content decreased from 24.9% to nearly zero, the tensile strength increased by 68% (up to 64.2 MPa). With the hemicellulose content from 6.8% to 20.4%, the tensile strength increased by 267% (up to 79.0 MPa).

The changes in the tensile strength of SNFM can be summarized into three stages during the progressive lignin and hemicellulose removal process. Two linear functions (i.e., tensile strength vs. lignin content) for Pr-DFs were curve-fitted with high correlations as shown in Fig. 7a, exhibiting a slow change from 38.2 to 41.9 MPa (ca. 10% increment) between 24.9% and 13.1% lignin contents, and a rapid increase from 41.9 to 64.2 MPa (ca. 53% increment) between 13.1% and 0.0% lignin content. One linear function (i.e., tensile strength vs. hemicellulose content) for Pr-HFs (Fig. 7b) was obtained, demonstrating a rapid decrease with the decreasing hemicellulose content.

The self-bonded process can be explained that the inter-fiber bonding strength worked as a decisive role in the tensile strength for the high-performance SNFM products, but which was based on a well-maintained fiber cell wall structure for the lignin etching process. However, for the hemicellulose etching process, the tensile strength was mainly determined by the strength of single fibers rather than the inter-fiber bonding, which can be seen from the results (Figs. 4g–h and 7b) that the destructions of fiber structure caused the decrease in tensile strength, although the inter-fiber compactness was increased.

3.8. Comparison of mechanical performances among SNFM products, plastic and natural wood

A high-performance SNFM product was developed in this work as a promising alternative to plastic and natural wood. The comparison of mechanical strengths among SNFM products, plastic, and natural wood is listed in Table 2. It can be seen that the tensile strength (TS) and flexural strength (FS) of SNFM products can reach 83.5 MPa and 127.3 MPa, respectively, which is much higher than plastics

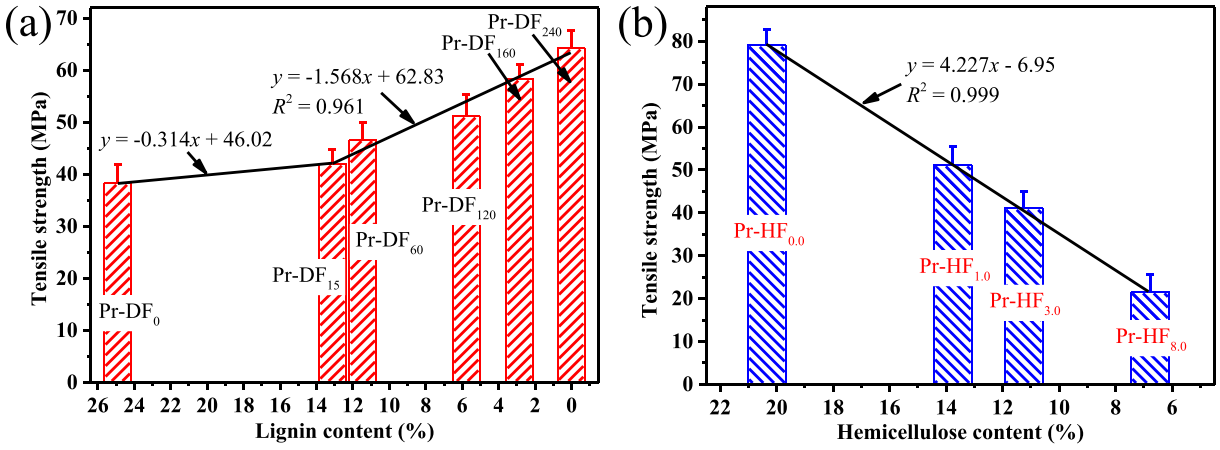

Fig. 7. Effects of (a) lignin content on Pr-DFs and (b) hemicellulose content on Pr-HFs in tensile strength.

(TS: 51.0 MPa; FS: 73.0 MPa) and natural wood (TS: 55.6 MPa; FS: 92.4 MPa). Moreover, compared with plastics (TS: 15.9–51.0 MPa; FS: 21.7–73.0 MPa) and natural wood (TS: 46.5–55.6 MPa; FS: 70.7–92.4 MPa), the SNFM products exhibited a tunable mechanical performance in larger ranges of 21.5–83.5 MPa (TS) and 31.2–127.3 MPa (FS). Meanwhile, similar density is presented for the SNFM products (0.86–1.06 g cm^{-3}) and plastics (0.89–1.03 g cm^{-3}) except for natural wood. It was worthy of noting that the new-prepared SNFM products also showed super higher mechanical strength than traditional molded pulp products. Thus, the high-performance SNFM products have great potential to replace plastic and natural wood for applications in buildings and other fields.

4. Conclusions

We developed a high-performance self-bonded natural-fiber material (SNFM), which showed much higher mechanical strength than natural wood and plastics (e.g., HDPE, PP, PVC, and ABS). The mechanical property enhancement of SNFM was achieved by modifying the plasticity and structures of fiber cell walls. The fiber plasticity can be tuned by controlling the mat moisture content during compression molding process. The cell wall structures can be etched by a progressive chemical treatment, in which, the surface and internal lignin was removed separately using sodium chlorite, and the hemicellulose was etched by microwave-assisted formic acid extraction. The mechanical properties of SNFM products were significantly improved (tensile strength: from 38.0 to 83.5 MPa; flexural strength: from 31.2 to 73.3 MPa) by increasing the fiber plasticity. The selective surface lignin removal dramatically increased the flexural strength from 101.3 to 122.1 MPa. Using the method of curve-fitting, linear functions between mechanical strength and lignin content, hemicellulose content, and mat moisture content were established with high correlations. The strength of single fibers played a more important role than the inter-fiber bonding in deciding the mechanical strength for the hemicellulose-etched material, which was contrary to the situation for the delignified products. It is of great significance to comprehensively understand the self-bonded mechanism for natural fiber materials.

Table 2
Mechanical properties of SNFM products, plastics, and natural woods.

Samples	Tensile strength (MPa)	Flexural strength (MPa)	Density (g cm^{-3})	Data sources
SNFM	21.5–83.5	31.2–127.3	0.86–1.06	In this study
HDPE[a]	17.0	21.7	0.95	[37]
	19.5	23.9	0.95	[38]
	20.8	24.1	0.96	[39]
PP[b]	17.9	29.8	0.89	[40]
	24.5–35.9	36.8–38.0	–	[41,42]
	30.0	50.8	0.91	[43]
PVC[c]	15.9	26.5	–	[44]
	38.6	67.1	–	[45]
	41.3–42.0	65.3–73.0	–	[46–48]
ABS[d]	42.8	62.0	1.03	[49]
	49.6	42.7	–	[50]
	51.0	61.5	–	[51]
Poplar	55.6 ± 8.0	92.4 ± 10.2	–	[52–54]
Cedar	46.5 ± 5.4	70.7 ± 10.2	0.5	
TMP[e]	0.5–1.3	–	0.12–0.15	[8]
	4.1–4.4	–	0.35	[55]
	8.8–17.1	–	0.52–0.80	[13]

Notes:
[a] HDPE: high density polyethylene.
[b] PP: polypropylene.
[c] PVC: polyvinyl chloride.
[d] ABS: acrylonitrile butadiene styrene.
[e] TMP: traditional molded pulp products.

CRediT authorship contribution statement

Quanliang Wang: Design, Execution, Data curation, Writing - original draft. Shengling Xiao, Sheldon Q. Shi, and Liping Cai: Review & editing, Supervision.

Acknowledgments

This work was supported by the National Key R&D Program of China (No. 2017YFD0601004) and the Applied Technology Research and Development Project of Harbin (No. 2016RAXXJ004).

Data availability

Raw/processed data required to reproduce these findings cannot be shared at this time due to technical or time limitations.

References

[1] Q. Wang, S. Xiao, S.Q. Shi, L. Cai, Effect of light-delignification on mechanical, hydrophobic, and thermal properties of high-strength molded fiber materials, Sci. Rep. 8 (2018) 955–964.
[2] M.S. Meddah, M. Bencheikh, Properties of concrete reinforced with different kinds of industrial waste fibre materials, Constr. Build. Mater. 23 (2009) 3196–3205.
[3] C. Xia, S.Q. Shi, Y. Wu, L. Cai, High pressure-assisted magnesium carbonate impregnated natural fiber-reinforced composites, Ind. Crop. Prod. 86 (2016) 16–22.
[4] K.L. Pickering, M.G. Efendy, T.M. Le, A review of recent developments in natural fibre composites and their mechanical performance, Compos. Part A 83 (2016) 98–112.
[5] M.R. Sanjay, P. Madhu, M. Jawaid, P. Senthamaraikannan, S. Senthil, S. Pradeep, Characterization and properties of natural fiber polymer composites: a comprehensive review, J. Clean. Prod. 172 (2018) 566–581.

[6] C. Zhou, S.Q. Shi, Z. Chen, L. Cai, L. Smith, Comparative environmental life cycle assessment of fiber reinforced cement panel between kenaf and glass fibers, J. Clean. Prod. 200 (2018) 196–204.
[7] Q. Wang, S. Xiao, S.Q. Shi, L. Cai, Mechanical strength, thermal stability, and hydrophobicity of fiber materials after removal of residual lignin, BioResources 13 (2017) 71–85.
[8] S.F. Curling, N. Laflin, G.M. Davies, G.A. Ormondroyd, R.M. Elias, Feasibility of using straw in a strong, thin, pulp moulded packaging material, Ind. Crop. Prod. 97 (2017) 395–400.
[9] Y. Huang, B. Fei, P. Wei, C. Zhao, Mechanical properties of bamboo fiber cell walls during the culm development by nanoindentation, Ind. Crop. Prod. 92 (2016) 102–108.
[10] N. Okuda, K. Hori, M. Sato, Chemical changes of kenaf core binderless boards during hot pressing (II): effects on the binderless board properties, J. Wood Sci. 52 (2006) 249–254.
[11] C. Xia, S.Q. Shi, L. Cai, S. Nasrazadani, Increasing inorganic nanoparticle impregnation efficiency by external pressure for natural fibers, Ind. Crop. Prod. 69 (2015) 395–399.
[12] M. Suchy, E. Kontturi, T. Vuorinen, Impact of drying on wood ultrastructure: similarities in cell wall alteration between native wood and isolated wood-based fibers, Biomacromolecules 11 (2010) 2161–2168.
[13] Q.L. Wang, J.Q. Yue, S.L. Xiao, X.Z. Lu, Effects of initial moisture contents on properties of overloaded molded fiber materials under hot pressing conditions, J. Chem. Eng. Chin. Univ. 31 (2017) 951–959.
[14] T.Y.A. Fahmy, F. Mobarak, Advanced binderless board-like green nanocomposites from undebarked cotton stalks and mechanism of self-bonding, Cellulose 20 (2013) 1453–1457.
[15] N. Ayrilmis, T. Dundar, A. Kaymakci, F. Ozdemir, H.K. Jin, Mechanical and thermal properties of wood-plastic composites reinforced with hexagonal boron nitride, Polym. Compos. 35 (2013) 194–200.
[16] Y. Kojima, A. Kawabata, H. Kobori, S. Suzuki, H. Ito, R. Makise, M. Okamoto, Reinforcement of fiberboard containing lingo-cellulose nanofiber made from wood fibers, J. Wood Sci. 62 (2016) 1–8.
[17] K. Umemura, O. Sugihara, S. Kawai, Investigation of a new natural adhesive composed of citric acid and sucrose for particleboard, J. Wood Sci. 59 (2013) 203–208.
[18] J. Su, L. Zhang, W. Batchelor, G. Garnier, Paper engineered with cellulosic additives: effect of length scale, Cellulose 21 (2014) 2901–2911.
[19] X. Shen, J. Jia, C. Chen, Y. Li, J.K. Kim, Enhancement of mechanical properties of natural fiber composites via carbon nanotube addition, J. Mater. Sci. 49 (2014) 3225–3233.
[20] M.L. Loong, D. Cree, Enhancement of mechanical properties of bio-resin epoxy/flax fiber composites using acetic anhydride, J. Polym. Environ. 26 (2018) 224–234.
[21] A.Q. Dayo, Y.L. Xu, A. Zegaoui, A.A. Nizamani, J. Wang, L. Zhang, W.B. Liu, A.H. Shah, Reinforcement of waste hemp fibres in aromatic diamine-based benzoxazine thermosets for the enhancement of mechanical and thermomechanical properties, Plast. Rubber Compos. 46 (2017) 442–449.
[22] H. Wang, G. Xian, H. Li, Grafting of nano-TiO_2 onto flax fibers and the enhancement of the mechanical properties of the flax fiber and flax fiber/epoxy composite, Compos. Part A 76 (2015) 172–180.
[23] R. Hu, J.K. Lim, Fabrication and mechanical properties of completely biodegradable hemp fiber reinforced polylactic acid composites, J. Compos. Mater. 41 (2007) 1655–1669.
[24] Q. Wang, S. Xiao, S.Q. Shi, L. Cai, The effect of delignification on the properties of cellulosic fiber material, Holzforschung 72 (2018) 443–449.
[25] F. Chen, Z. Jiang, G. Wang, H. Li, L.M. Simth, S.Q. Shi, The bending properties of bamboo bundle laminated veneer lumber (BLVL) double beams, Constr. Build. Mater. 119 (2016) 145–151.
[26] D. Topgaard, O. Söderman, Changes of cellulose fiber wall structure during drying investigated using NMR self-diffusion and relaxation experiments, Cellulose 9 (2002) 139–147.
[27] J.R. Barnett, V.A. Bonham, Cellulose microfibril angle in the cell wall of wood fibres, Biol. Rev. 79 (2004) 461–472.
[28] M. KačUráková, P. Capek, V. Sasinková, N. Wellner, A. Ebringerová, FT-IR study of plant cell wall model compounds: pectic polysaccharides and hemicelluloses, Carbohyd, Polym. 43 (2000) 195–203.
[29] S. Iwamoto, K. Abe, H. Yano, The effect of hemicelluloses on wood pulp nanofibrillation and nanofiber network characteristics, Biomacromolecules 9 (2008) 1022–1026.
[30] S. Shao, Z. Jin, G. Wen, K. Iiyama, Thermo characteristics of steam-exploded bamboo (Phyllostachys pubescens) lignin, Wood Sci. Technol. 43 (2009) 643–652.
[31] Q. Tarrés, N.V. Ehman, M.E. Vallejos, M.C. Area, M. Delgado-Aguilar, P. Mutjé, Lignocellulosic nanofibers from triticale straw: the influence of hemicelluloses and lignin in their production and properties, Carbohyd. Polym. 163 (2017) 20–27.
[32] Y.Y. Liu, M.R. Liu, H.L. Li, B.Y. Li, C.H. Zhang, Characteristics of high yield pulp fibers by xylanase treatment, Cellulose 23 (2016) 1–9.
[33] L. Segal, J.J. Creely, A.E.M. Jr, C.M. Conrad, An empirical method for estimating the degree of crystallinity of native cellulose using the X-ray diffractometer, Text. Res. J. 29 (1959) 786–794.
[34] A. Leszczyńska, K. Stafin, J. Pagacz, M. Mičušík, M. Omastova, E. Hebda, J. Pielichowski, D. Borschneck, J. Rose, K. Pielichowskia, The effect of surface modification of microfibrillated cellulose (MFC) by acid chlorides on the structural and thermomechanical properties of biopolyamide 4.10 nanocomposites, Ind. Crop. Prod. 116 (2018) 97–108.
[35] D.M. Panaitescu, A.N. Frone, I. Chiulan, A. Casarica, C.A. Nicolae, M. Ghiurea, R. Trusca, C.M. Damiand, Structural and morphological characterization of bacterial cellulose nano-reinforcements prepared by mechanical route, Mater. Design. 110 (2016) 790–801.
[36] R.H. Newman, Carbon-13 NMR evidence for cocrystallization of cellulose as a mechanism for hornification of bleached kraft pulp, Cellulose 11 (2004) 45–52.
[37] Y. Lei, Q. Wu, C.M. Clemons, F. Yao, Y. Xu, Influence of nanoclay on properties of HDPE/wood composites, J. Appl. Polym. Sci. 106 (2010) 958–966.
[38] H. Sepet, N. Tarakcioglu, R. Misra, Investigation of mechanical, thermal and surface properties of nanoclay/HDPE nanocomposites produced industrially by melt mixing approach, J. Compos. Mater. 50 (2015) 218–224.
[39] S. Mohanty, S.K. Nayak, Interfacial, dynamic mechanical, and thermal fiber reinforced behavior of MAPE treated sisal fiber reinforced HDPE composites, J. Appl. Polym. Sci. 102 (2010) 3306–3315.
[40] M.B. Abu Bakar, Y.M. Leong, A. Ariffin, Z.A. Mohd. Ishak, Mechanical, flow, and morphological properties of talc-and kaolin-filled polypropylene hybrid composites, J. Appl. Polym. Sci. 104 (2010) 434–441.
[41] G. Toriz, F. Denes, R.A. Young, Lignin-polypropylene composites. part 1: composites from unmodified lignin and polypropylene, Polym. Compos. 23 (2010) 806–813.
[42] S.K. Chattopadhyay, R.K. Khandal, R. Uppaluri, A.K. Ghoshal, Bamboo fiber reinforced polypropylene composites and their mechanical, thermal, and morphological properties, J. Appl. Polym. Sci. 119 (2010) 1619–1626.
[43] J.Z. Liang, Tensile and flexural properties of polypropylene composites filled with highly effective flame retardant magnesium hydroxide, Polym. Test. 60 (2017) 110–116.
[44] X. Xu, L. Wang, H. Toghiani, C.U. Pittman, Effect of crosslinking on mechanical and viscoelastic properties of semiinterpenetrating polymer networks composed of poly(vinyl chloride) and isocyanate crosslinked networks, J. Appl. Polym. Sci. 78 (2000) 1402–1411.
[45] J. Prachayawarakorn, J. Khamsri, K. Chaochanchaikul, N. Sombatsompop, Effects of compatibilizer type and rubber-wood sawdust content on the mechanical, morphological, and thermal properties of PVC/LDPE blend, J. Appl. Polym. Sci. 102 (2010) 598–606.
[46] X.F. Zeng, W.Y. Wang, G.Q. Wang, J.F. Chen, Influence of the diameter of $CaCO_3$ particles on the mechanical and rheological properties of PVC composites, J. Mater. Sci. 43 (2008) 3505–3509.
[47] S.A. Bahari, W.J. Grigsby, A. Krause, Flexural properties of PVC/bamboo composites under static and dynamic-thermal conditions: effects of composition and water absorption, Int. J. Polym. Sci. 2017 (2017) 1–8.
[48] H. Zhao, R. Sun, Y. Luo, J. Li, A novel method of hyperbranched poly(amide-ester) modifying nano-SiO2 and study of mechanical properties of PVC/nano-SiO_2 composites, Polym. Compos. 29 (2010) 1014–1019.
[49] S.P. Jang, D. Kim, Thermal, mechanical, and diffusional properties of nylon 6/ABS polymer blends: compatibilizer effect, Polym. Eng. Sci. 40 (2010) 1635–1642.
[50] Z. Weng, J. Wang, T. Senthil, L. Wu, Mechanical and thermal properties of ABS/montmorillonite nanocomposites for fused deposition modeling 3D printing, Mater. Design 102 (2016) 276–283.
[51] J. Dong, C. Zhao, Z. Tan, S. Li, Z. Fan, Structure and properties of heat-resistant ABS resins innovated by NSM random copolymer, Polym. Compos. 34 (2013) 920–928.
[52] J. Song, C. Chen, S. Zhu, M. Zhu, J. Dai, U. Ray, et al., Processing bulk natural wood into a high-performance structural material, Nature 554 (2018) 224–228.
[53] T.T.H. Nguyen, S. Li, J. Li, The combined effects of copper sulfate and rosin sizing agent treatment on some physical and mechanical properties of poplar wood, Constr. Build. Mater. 40 (2013) 33–39.
[54] T.H. Yang, F.R. Chang, C.J. Lin, F.C. Chang, Effects of temperature and duration of heat treatment on the physical, surface, and mechanical properties of Japanese cedar wood, BioResources 11 (2016) 3947–3963.
[55] S.P. Gurav, A. Bereznitski, A. Heidweiller, P.V. Kandachar, Mechanical properties of paper-pulp packaging, Compos. Sci. Technol. 63 (2003) 1325–1334.